Bone matrix quality in paired iliac bone biopsies from postmenopausal women treated for 12 months with strontium ranelate or alendronate

Guillaume Falgayrac, Delphine Farlay, Camille Ponçon, Hélène Béhal, Marc Gardegaront, Patrick Ammann, Georges Boivin, Bernard Cortet

Bone matrix quality in paired iliac bone biopsies from postmenopausal women treated for 12 months with strontium ranelate or alendronate.

Guillaume Falgayrac[1], Delphine Farlay[2], Camille Ponçon[2], Hélène Béhal[4], Marc Gardegaront[2], Patrick Ammann[3], Georges Boivin[2], Bernard Cortet[1]

Affiliations

[1] Univ. Lille, CHU Lille, Univ. Littoral Côte d'Opale, ULR 4490 - MABLab, F-59000 Lille, France

[2] INSERM, UMR1033, Univ Lyon, Université Claude Bernard Lyon1, Lyon France

[3] Division of Bone Diseases, Department of Internal Medicine Specialties, Geneva University Hospital, 4, rue Gabrielle-Perret-Gentil, CH-1211 Geneva 14, Switzerland

[4] Univ. Lille, CHU Lille, ULR 2694 - METRICS: Évaluation des technologies de santé et des pratiques médicales, F-59000 Lille, France

Corresponding author: guillaume.falgayrac@univ-lille.fr

Guillaume FALGAYRAC
MABLab ULR4490
Faculty of Dentistry
Place de Verdun
59000 Lille FRANCE

1 Highlights

- A large number of paired bone biopsies (n=60) were studied
- Alendronate increases mineralization and crystallinity in new bone
- Alendronate increases the relative amount of proteoglycan in new bone
- Strontium ranelate decreases carbonate content and crystallinity
- Strontium promotes bonds with collagen and noncollagenous proteins

Keywords: Mineralization – Collagen – Bone Quality – Alendronate – Strontium – Paired Human Bone Biopsies

2 Abstract

Bone quality is altered mainly by osteoporosis, which is treated with modulators of bone quality. Knowledge of their mechanisms of action is crucial to understand their effects on bone quality. The goal of our study was to compare the action of alendronate (ALN) and strontium ranelate (SrRan) on the determinants of bone quality. The investigation was performed on over 60 paired human iliac biopsies. Paired samples correspond to biopsies obtained from the same patient, one before treatment (baseline) and one after 12 months of treatment, in postmenopausal women with osteoporosis. Vibrational spectroscopy (Raman and FTIRM) and nanoindentation were used to evaluate the effect of both drugs on bone quality at the ultrastructural level. Outcomes measured by vibrational spectroscopy and nanoindentation are sensitive to bone age. New bone packets are distinguished from old bone packets. Thus, the effect of bone age is distinguished from the treatment effect. Both drugs modify the mineral and organic composition in new and old bone in different fashions after 12 months of administration. The new bone formed during ALN administration is characterized by an increased mineral content, carbonation and apatite crystal size/perfection compared to baseline. Post-translational modifications of collagen are observed through an increase in the hydroxyproline/proline ratio in new bone. The proteoglycan content is also increased in new bone. SrRan directly modulates bone quality through its physicochemical actions, independent of an effect on bone remodeling. Strontium cations are captured by the hydrated layer of the mineral matrix. The mineral matrix formed during SrRan administration has a lower carbonate content and crystallinity after 12 months than at baseline. Strontium might create bonds (crosslinks) with collagen and noncollagenous proteins in new and old bone. The nanomechanical properties of bone were not modified with either ALN or SrRan, probably due to the short duration of administration. Our results show that ALN and SrRan have differential effects on bone quality in relation to their mechanism of action.

3 Introduction

The term “bone quality” describes the composition and architectural properties of bone, which determine its material and mechanical properties [1]. Bone quality is altered by bone diseases. Modulators of bone quality are used to treat bone diseases, particularly osteoporosis. Knowledge of their molecular mechanisms is crucial to obtain an understanding of their effects on bone quality.

Bisphosphonates (BPs) have been used for many years as antiresorptive agents for treating bone diseases, particularly osteoporosis. Among the different BPs available, alendronate (ALN) is the most commonly used for the treatment of postmenopausal osteoporosis (PMOP) [2]. The mechanism of action of ALN as an antiresorptive drug acting on osteoclasts is well known [3]. ALN decreases bone resorption by inhibiting osteoclast formation and function [4]. The effect of ALN on bone quality at the ultrastructural level has been the subject of several studies involving animal models and humans. In studies involving human samples and ALN treatment, the duration therapy covered a range of treatments from 2 to 10 years. For short-term ALN treatment (2-3 years), microradiography, quantitative backscattered electron imaging (qBEI) and vibrational spectroscopy showed an increase in the mineral composition and a decrease in the spatial heterogeneity of the bone material properties [5-7]. For long-term treatment (3-10 years), vibrational spectroscopy and qBEI analysis did not reveal modification of the mineral and the organic composition at similar bone ages [8-10]. A decrease in the heterogeneity of the bone material properties was observed in the long-term treatment [11, 12]. Tissue hardness was also reduced after long-term ALN treatment compared to a placebo [12].

Among all available anti-osteoporotic agents, there is a drug that is not considered an anabolic or anticabolic agent: strontium ranelate (SrRan). The mechanism of action of Sr^{2+} from SrRan on bone is still being debated [13]. However, studies agree that Sr^{2+} is fixed in newly formed bone packets during treatment. There is no diffusion from newly formed bone packets into old bone packets [14-16]. Three hypotheses are accepted regarding the location of Sr^{2+} in bone mineral. (i) Sr is adsorbed at the surface of collagen or bone mineral. Sr may have different coordination numbers with surrounding oxygen atoms; (ii) a slower mechanism of heteroionic substitution occurs, which results in the incorporation of strontium into the crystal lattice replacing calcium in site (I) or (II); and (iii) Sr is in the hydrated region of the bone mineral [17, 18]. The effect of SrRan treatment on human bone quality at the microstructural level was investigated in human samples. The duration therapy covered a range of treatments from 6 months to 8 years. All studies agree about the effect of SrRan on bone properties in human samples. The maximum amount of Sr fixed in bone reaches less than 1.6% (%wt)Sr/(Sr+Ca) after 3 years of administration [19, 20]. Vibrational spectroscopy, microradiography, qBEI, small-angle scattering and X-

ray diffraction showed no modification of the mineral and collagen cross-links after 3 years of treatment [14, 15]. Bone mechanical properties, assessed by nanoindentation, showed no difference between patients treated with SrRan for 3 years versus a placebo [15]. In a comparative study between SrRan and ALN, histomorphometric analyses showed that bone formation remained higher with a lower diminution of bone remodeling with SrRan versus ALN [21]. The present study is a follow-up of these histomorphometric analyses [21].

Our study aimed to compare bone quality changes induced by two anti-osteoporotic treatments (ALN and SrRan), which each have their own characteristic mechanism of action. Vibrational spectroscopy and nanoindentation assessments were performed to evaluate their effects on the mineral and organic matrix of bone at the ultrastructural level. Vibrational spectroscopy techniques (Raman and Fourier transform infrared microscopy, FTIRM) were used to study bone at the molecular level [22]. Both techniques are complementary and describe the molecular composition of mineral and organic components through physicochemical variables (PPVs). The nanoindentation technique assesses the tissue hardness, elastic modulus and working energy at the scale of a single BSU. Our study will provide insights into the differential effect of ALN and SrRan on bone quality in the short term at the ultrastructural level.

4 Materials and methods

4.1 Bone samples

Paired iliac bone biopsies (n=60) were provided by the Institut de Recherches Internationales Servier (Suresnes, France). These biopsies were obtained from a subset of a double-blind study comparing the effects of SrRan and ALN on bone histomorphometry [21]. Sixty pairs of bone biopsies (30 pairs SrRan and 30 pairs ALN) were randomly selected among the 387 pairs of bone biopsies from the initial phase III study [21]. The characteristics of the menopausal women (average age, femoral neck BMD T-score, total hip BMD T-score, lumbar L1-L4 BMD T-score and time since menopause) are described in Table 1. Briefly, the 60 osteoporotic women were 50 and 76 years old and were menopausal for at least 3 years. The ALN group had an average age of 64.4 years, and the SrRan group had an average age of 63.3 years. No statistically significant difference was found between the ALN and SrRan groups regarding the main characteristics of the population. A first transiliac bone biopsy was performed with a 7.5-mm inner diameter trephine in all patients at baseline. A second bone biopsy specimen was collected from the opposite side after 12 months of administration. The dosing regimen was set at 2 g per day for SrRan and 70 mg once a week for ALN. The 60 paired biopsies were divided into 2 groups

according to the treatment administered: ALN and SrRan. Each group included 30 paired samples. A paired sample corresponded to a biopsy obtained from the same patient at baseline (M0) and a biopsy obtained after 12 months of treatment (M12). After fixation with 70% ethanol and dehydration in 100% ethanol, biopsies were embedded in polymethylmethacrylate (PMMA). Each block of PMMA was cut into 5 parts with specific thicknesses adapted to the technique of analysis. Three of 5 parts were used in the present study: the approach part, a 2 µm-thick part and the remaining part (Figure 1 a, d and e). The 3 parts were not stained.

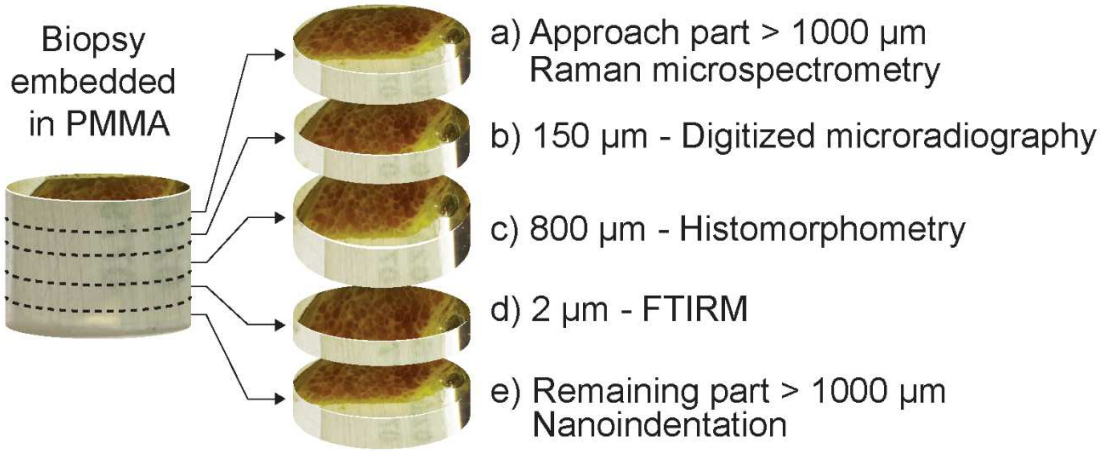

Figure 1: Each embedded biopsy was cut into 5 parts with a specific thickness adapted to the technique of analysis. a) For the "approach part", the thickness was greater than 1000 µm and dedicated to Raman microspectrometry. b) The thickness was ~ 150 µm and dedicated to digitized microradiography. The results of this technique are not included in the actual article. c) The thickness was ~ 800 µm and dedicated to histomorphometry. The results are presented in the article by Chavassieux *et al* [21]. d) The thickness was ~ 2 µm and dedicated to FTIRM analysis. e) The thickness was greater than 1000 µm and dedicated to nanoindentation analysis.

The samples were divided into 2 sets. The first set was used for vibrational spectroscopic analysis and included 30 paired samples per treatment. For the FTIRM analysis, undecalcified parts (2 µm thick) were cut from the first set with a Polycut E microtome (Reichert-Jung, Leica, Germany) and stored between 2 slides. Raman microspectroscopy was performed on the "approach part". The surface was polished using abrasive paper with decreasing grains (30, 12, 3 and 0.3 µm). The second set was composed of the remaining parts and analyzed by nanoindentation. During the time frame of this study, only 19 paired bone biopsies per treatment were analyzed because nanoindentation was time consuming. Sections of biopsies were polished, finished with a 0.25 mm diamond solution, and rehydrated in a saline solution for 12 hours at 22°C using a standard protocol. The design of the study is presented in Figure 2.

Table 1: Averaged characteristics of the patients at baseline. The comparison of the characteristics of both groups was performed with a t-test. There was no difference between the groups according to age, femoral neck BMD T-score, total hip BMD T-score, lumbar L1-L4 BMD T-score or the time since menopause.

	ALN	SrRan	p-value
Age (years)	64.4 (±6.35)	63.3 (±7.77)	0.57
Femoral neck BMD T-score	-2.14 (±0.71)	-2.07 (±0.63)	0.71
Total hip BMD T-score	-1.73 (±0.86)	-1.49 (±0.75)	0.25
Lumbar L1-L4 BMD T-score	-2.96 (±0.81)	-2.74 (±0.65)	0.26
Time since menopause (years)	16.24 (±6.73)	13.84 (±7.61)	0.20
Demographic origin (n [%])			
North America	14 [23]	12 [20]	
South America	1 [2]	2 [3]	
Europe	15 [25]	16 [27]	

BMD= Bone Mineral Density.

Values are expressed as means with standard deviation (±SD) or percentage (n[%]) of the total number of biopsies (n=60).

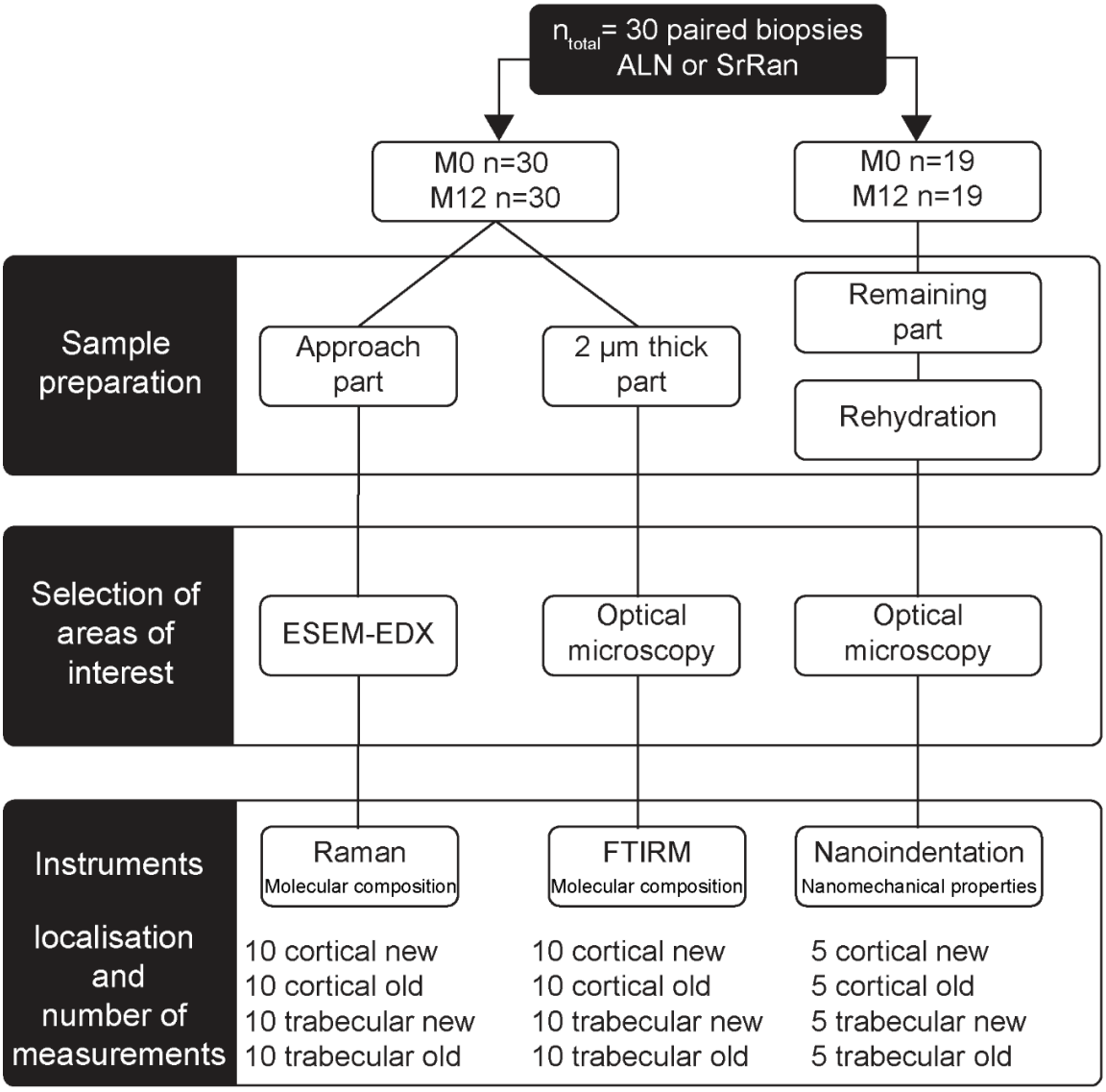

Figure 2: Description of the design of the study for each treatment (ALN or SrRan). Each treatment was composed of 30 paired biopsies embedded in PMMA. A paired biopsy corresponds to a biopsy at baseline (before the treatment, M0) and a biopsy after 12 months (M12) of administration of ALN or SrRan. Group M0 was composed of 30 biopsies, and group M12 was composed of 30 biopsies. Each biopsy was cut into 5 parts (Figure 1), and 3 parts were analyzed in this work. The approach parts were imaged by environmental scanning electron microscopy coupled with energy dispersive X-ray (ESEM-EDX) to distinguish new from old bone packets. All paired approach parts (n=30) were analyzed by Raman microspectroscopy. The 2 µm-thick parts were observed by optical microscopy to distinguish new from old bone packets. All paired 2 µm-thick parts (n=30) were analyzed by FTIRM. The remaining paired parts were observed by optical microscopy to distinguish new from old bone packets. Nineteen of the 30 paired remaining parts were rehydrated and analyzed by nanoindentation.

4.2 Raman spectroscopy and physicochemical variables

The Raman spectrometer was a LabRAM HR800 (HORIBA, Jobin-Yvon, France). The acquisition time per spectrum was the average of 4 acquisitions of 30 seconds each (120 sec in total). The laser wavelength was 785 nm and the laser power output was 100 mW. The DuoScan mode was set to scan a

surface of 30×30 μm^2 to ensure a similar spatial resolution as the FTIRM analysis [23]. One Raman spectrum corresponds to one bone packet. Five spectra were acquired on 5 different new bone packets from each cortical region (left and right). Ten spectra were acquired from 10 different new trabecular bone packets. A total of 20 spectra (10 cortical and 10 trabecular) were acquired in new bone packets for each sample. The same acquisition protocol was repeated on the old bone packets from each biopsy, resulting in 20 measurements of old bone (10 cortical and 10 trabecular). The localization procedure is detailed in section 4.5 (Figure 3). After the acquisition, a Savitzky−Golay smoothing filter (filter width: 3; and polynomial order: 2) was applied to all Raman spectra. The intensities and areas were integrated over defined Raman shift regions in the spectrum using a sum filter. The filter calculates the intensities and areas within the chosen borders, and the background is subtracted by taking a local piecewise linear baseline from the first to the second border [24]. Six physicochemical variables (PPVs) were calculated for each spectrum [25, 26]: the mineral/organic ratio = ratio of area of ν_1PO_4 (960 cm^{-1}, peak-ROI 900-990 cm^{-1}) to the area of $\delta(CH_2)$ (1450 cm^{-1}, peak-ROI 1434 -1490 cm^{-1}); carbonation type-B = ratio of area of type-B CO_3^{2-} (1070 cm^{-1}, peak-ROI 1052–1092 cm^{-1}) and area of ν_1PO_4; crystallinity, the full width at half maximum intensity (FWHM) of ν_1PO_4; the hydroxyproline/proline ratio = ratio of intensity of hydroxyproline (875 cm^{-1}, peak-ROI 828-898 cm^{-1}) and intensity of proline (855 cm^{-1}, peak-ROI 828-898 cm^{-1}); collagen maturity = ratio of the intensity of 1660 cm^{-1} (peak-ROI 1615 -1705 cm^{-1}) and intensity of 1690 cm^{-1} (peak-ROI 1615 -1705 cm^{-1}) [27]; and the relative proteoglycan (PG) content = ratio of areas of PG (peak-ROI 1365–1390 cm^{-1}) to the area of amide III band (peak-ROI 1243–1269 cm^{-1}) [28]. An example of a raw Raman spectrum with bands assignments and local piecewise linear baseline is shown in the supplementary file (Figure S1-a).

4.3 FTIRM and physicochemical variables

FTIRM analysis was performed in transmission mode on 2 µm-thick sections with a Spectrum 100 spectrometer coupled with an AutoImage GXII microscope (PerkinElmer GXII Auto-image Microscope) equipped with a wideband detector (mercury–cadmium–telluride) (7800–400 cm_{-1}). Each spectrum was collected at a 45 × 35 μm^2 spatial resolution with a 4 cm^{-1} spectral resolution and an average of 50 scans. The contributions of air and PMMA (by nullifying the main peak of PMMA at 1730 cm^{-1}) were subtracted from each raw spectrum, and the baseline (quadratic function) was corrected. An example of a raw and corrected spectra with the assignment of bands is shown in the supplementary file (Figure S1-b). Each measurement was performed on both new cortical and trabecular bone samples. Similar to Raman analysis, one FTIRM spectrum corresponds to one bone packet. Five acquisitions were performed on 5 different new bone packets from each cortical region (left and right). Ten spectra were acquired from 10

different new trabecular bone packets. A total of 20 spectra (10 cortical and 10 trabecular) were acquired in new bone packets for each sample. The same acquisition protocol was repeated on the old bone packets from each biopsy, resulting in 20 measurements of old bone (10 cortical and 10 trabecular). The localization procedure is detailed in section 4.5 (Figure 4-a). Finally, each spectrum was deconvoluted by using the peak fitting method with GRAMS/AI software (Thermo Galactic, Salem, NH, USA). Regarding the $\nu_1\nu_3PO_4$ vibration, five subbands were used (1110, 1082, 1060, 1030, 962 cm^{-1}), and, for the ν_4PO_4 vibration, four subbands were used (604, 577, 563, 552 cm^{-1}). The amide I vibration was curve-fitted into 3 main components, 1690 cm^{-1}, 1660 cm^{-1} and 1633 cm^{-1}, and 6 other peaks corresponding to the other amide vibrations were added. For the amide vibration, a total of 9 peaks were fitted altogether [29-32]. Five variables were calculated per spectrum: mineral/organic ratio = ratio of the integrated area under the curve for $\nu_1\nu_3$ PO_4 (1184-910 cm^{-1}) and the integrated area under the curve for amide I (1730-1592 cm^{-1}); mineral maturity = ratio of the area under the curve for $\nu_1\nu_3$ PO_4 at 1030 cm^{-1} (apatitic phosphates) and the area under the curve for $\nu_1\nu_3$ PO_4 at 1110 cm^{-1} (nonapatitic phosphates); crystallinity = inverse of the width at the half-height of the peak at 604 cm^{-1} (ν_4PO_4); and carbonation= ratio of the integrated area under the curves for ν_2CO_3 (862-894 cm^{-1}) and $\nu_1\nu_3$ PO_4 (1184-910 cm^{-1}). FTIRM assesses the total carbonate contents (types A + B + labile), while Raman spectroscopy assesses the type-B carbonate contents. Collagen maturity is defined as the ratio of the area at 1660 cm^{-1} (amide I) to the area at 1690 cm^{-1} (amide I).

4.4 Nanomechanical properties: nanoindentation analysis

Nanoindentation tests were used to evaluate the material-level properties of bone tissue. The elastic modulus, tissue hardness, working energy and elastic energy of the bone were determined for rehydrated bone tissue samples. A nanohardness tester (NHT, CSM Instruments, Peseux, Switzerland) was used as follows: force-displacement data of a pyramidal diamond indenter that was pressed onto a material were recorded as previously described [33]. An original Berkovich tip with a three-sided pyramid characterized by a half angle of 65.3 degrees was used. The indenter tip was loaded at a given depth into the sample, and the load was then held constant, leading to creeping of the material below the tip. This results in a combination of elastic and postyield deformation, which is analyzed to obtain the elastic modulus and tissue hardness as well as the working energy. Tissue hardness is interpreted as the mean pressure that the material can resist and is calculated as the ratio of the maximum force to the contact area. The elastic modulus is defined by the initial slope of the unloading section of the curve. Finally, the working energy is calculated as the surface between the load-displacement curves, as well as the plastic and elastic energy. The details of the variables are presented in the supplementary files. The

sections of the human biopsies were polished and finished with a 0.25 mm diamond solution, and the samples were rehydrated following a standardized protocol in saline solution for 12 hours at 22 °C. The mechanical tests were conducted at locations comparable to those analyzed using Raman spectroscopy and FTIRM. One indent corresponds to one bone packet. Five indents were generated in 5 different cortical new bone packets (over left and right cortices). Five indents were generated in 5 different trabecular new bone packets. It represents a total of 10 indents in the new bone (5 cortical and 5 trabecular). The same procedure was performed in cortical and trabecular old bone. A total of 10 indents were obtained in old bone (5 cortical and 5 trabecular). The localization procedure is detailed in section 4.5 (Figure 4-d). The indents were set to a 900 nm depth with an approximate speed of 76 mN/min for both loading and unloading, and, at maximum load, a 10 second holding period was applied. Finally, the limit of the maximal allowable thermal drift was set to 0.1 nm/s.

4.5 Localization of areas with comparable bone age

Outcomes measured by vibrational spectroscopy (Raman and FTIRM) and nanoindentation are sensitive to bone age. Bone packets must be distinguished to compare bone areas with similar bone ages. Therefore, the effect of bone age is dissociated from the effect of the treatment. Initially, all patients received double tetracycline labeling before bone biopsies [21]. Unfortunately, the tetracycline labels were not clearly visible. Two procedures were performed to locate the bone areas depending on the bone age. Each procedure was adapted according to the sample preparation constraints.

The first procedure was based on an environmental scanning electron microscope coupled with an energy dispersive spectroscopy detector (ESEM-EDX). Prior to the acquisition of the Raman spectra, the biopsies were analyzed using ESEM-EDX. Back scattered electron images (BSE) were used to distinguish bone packets with comparable mineralization levels within each sample and thus comparable bone ages. Figure 3 illustrates an example of selected locations. Areas with a dark gray level were distinguished from areas with a light gray level in the ALN M0, ALN M12, and SrRan M0 samples. This distinction allowed us to identify recently formed bone packets (Figure 3-dark gray-red circles) and old interstitial bone packets (Figure 3-light gray-white circles) [34]. Elemental images of Sr^{2+} were acquired from SrRan M12 samples to locate bone packets in which Sr was fixed (Figure 3-d and e). The BSE images and the elemental images of Sr^{2+} were used as a guide for Raman analysis. Throughout the manuscript, the term “new bone” refers to recently formed bone packets, and the term “old bone” refers to old interstitial bone.

The second procedure was based on optical microscopy. Prior to FTIRM and nanoindentation analyses, optical microscopy was used to localize bone packets with similar bone ages. Bone packets with

similar bone ages have characteristic anatomical locations. The location of the bone packets was determined according to the following procedure and was used as a guide for FTIRM and nanoindentation analyses. Figure 4 illustrates an example of selected locations. In cortical bone, recently formed bone packets were located in the endosteal area (red circles and diamonds). Old interstitial bone packets were located in the middle of the cortical bone (white circles and diamonds). In trabecular bone, recently formed bone packets were located in the periphery (red circles and diamonds). Old interstitial bone packets were located in the middle of the trabeculae (white circles and diamonds).

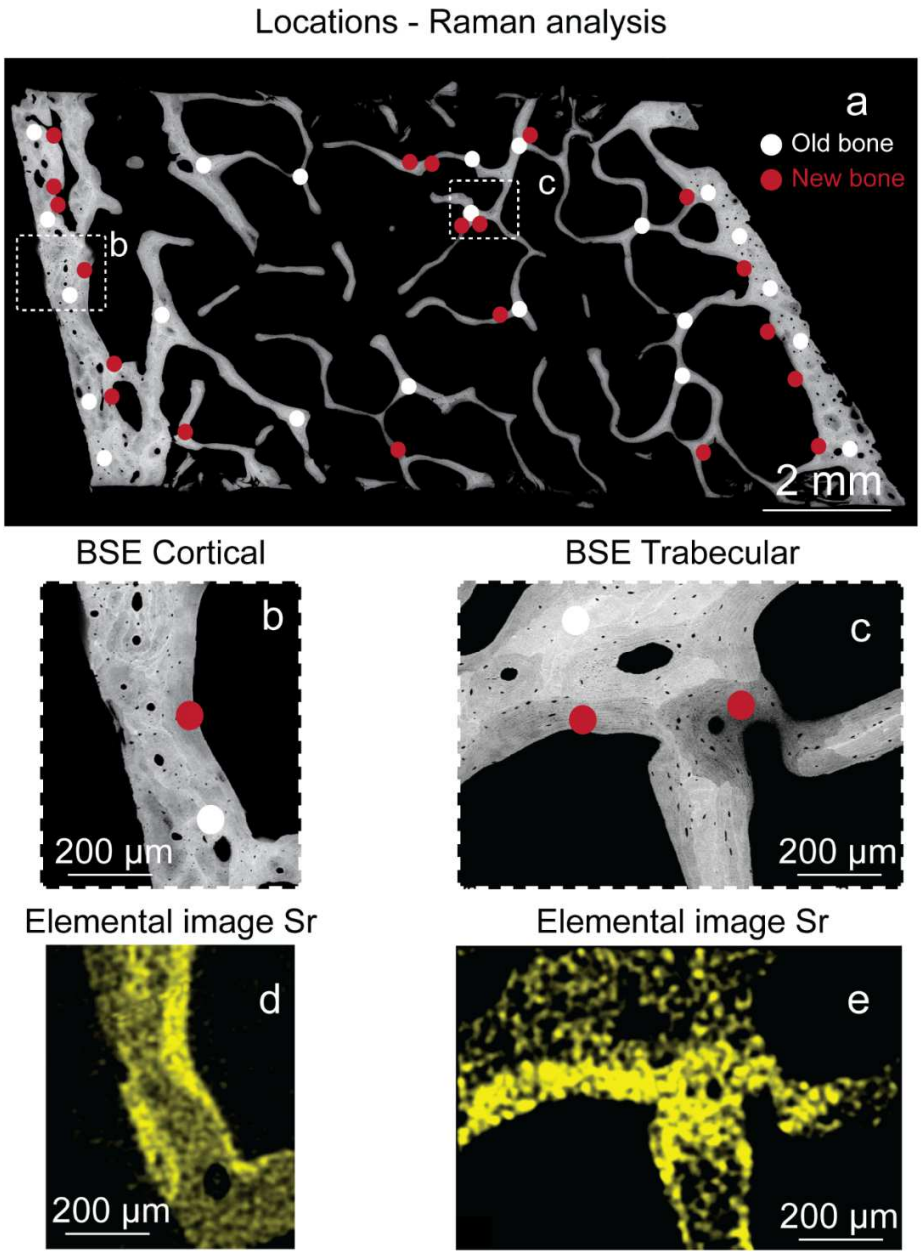

Figure 3: Example of localization of new and old bone packets analyzed by Raman spectroscopy. a) BSE image of an entire biopsy of the SrRan group. Circles in red and white represent new and old bone packets, respectively. Bone packets with dark gray correspond to a low level of mineralization (new bone), and bone packets with light gray correspond to a high level of mineralization (old bone). b and d) High magnification of a bone packet and the corresponding elemental image Sr in the cortical bone. c and e) High magnification of a bone packet and the corresponding elemental image Sr in the trabecular bone. In elemental image Sr, the area in strong yellow corresponds to the presence of Sr in new bone, and the area in light yellow corresponds to the noise. The BSE images and the elemental images Sr were used to guide Raman analysis.

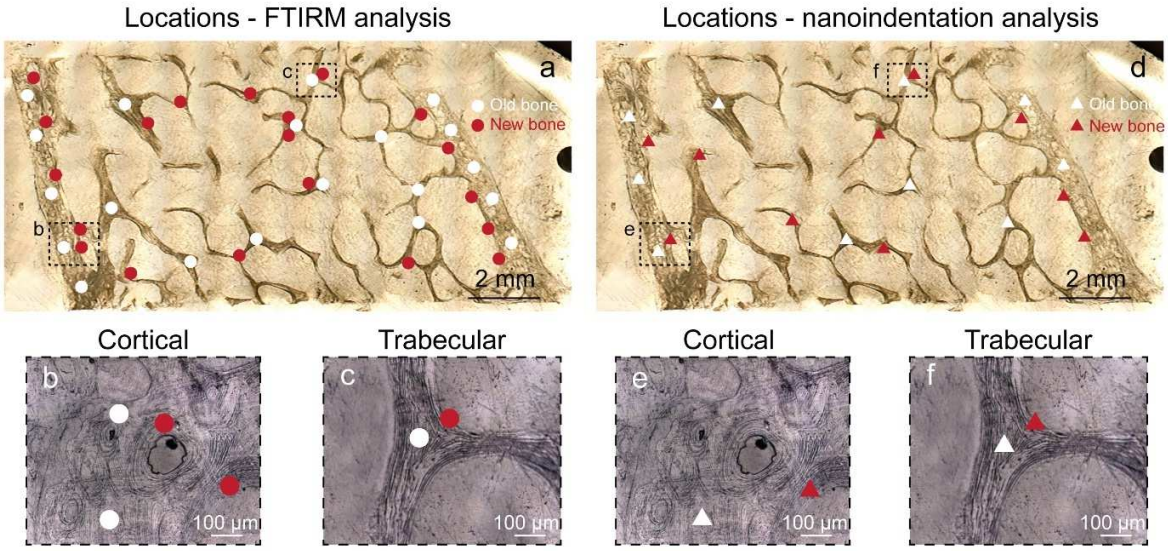

Figure 4: Example of the localization of new and old bone packets analyzed by FTIRM and nanoindentation. a) and d) optical image of an entire SrRan biopsy. Circles and diamonds represent examples of locations analyzed by FTIRM and nanoindentation, respectively. Magnification of a bone packet in b) cortical and c) trabecular bone for FTIRM analysis. Magnification of a bone packet in e) cortical and f) trabecular bone for nanoindentation analysis. The circles and diamonds in red represent locations of new bone. The circles and diamonds in white represent locations of old bone. Optical microscopy was used to guide FTIRM and nanoindentation analysis.

4.6 Bone sample quality analysis

The embedded biopsies were stored in the dark at ambient temperature [21]. Bone biopsies have been embedded for more than 5 years. Five elements were checked to evaluate whether long-term storage had an influence on the outcomes measured. First, the Raman and FTIRM spectra were in agreement with the reference spectra of bone. Second, the values of all PPVs were in agreement with PPVs from similar studies in the literature. Third, we also checked the coherence of the data when comparing PPVs according to the bone age (new bone versus old bone). The comparison of the well documented PPVs of new bone versus old bone gave results in agreement with the literature. PPVs such as the mineral/matrix ratio, carbonation and crystallinity were lower in new bone than in old bone. Fourth, EDX analysis confirmed the presence of Sr^{2+} in newly formed bone tissue after administration of SrRan. Fifth, the tissue hardness of bone is independent of the duration of embedding (article submitted).

4.7 Statistical analysis

The change in each physicochemical variable after 12 months were compared between the two treatments and the two locations using a linear mixed model (covariance pattern model) with treatment, location, treatment * location interaction and baseline value as fixed effects. The patients were

considered random effects. In the case of a significant interaction term, a post hoc comparison between treatments was performed. In the case of a nonsignificant interaction term, the same model was performed without the treatment * location interaction to estimate the treatment effect and the location effect.

Data were analyzed using SAS software (SAS Institute Inc., Cary, NC, USA), and all statistical tests were performed with a 2-tailed alpha risk of 0.05.

5 Results

The physicochemical variables (PPVs) were evaluated on new bone and old bone separately. The changes in the PPVs between baseline and after 12 months were compared according to the ALN or SrRan group. The Table 2 shows the averaged changes in PPVs in new bone independent of the location (cortical and trabecular). Statistical analysis revealed that only 2 of 15 PPVs were dependent on the location in new bone. Table 3 shows the averaged changes of both PPVs in new bone as a function of the location. Table 4 shows the averaged changes in the PPVs in old bone independent of the location. No PPVs were found to be dependent on the location in old bone. The effects of ALN and SrRan bone quality were evaluated by comparing the PPVs according to the bone age. Thus, the results and the discussion sections are presented according to the bone age (new bone and old bone).

5.1 Comparison of the results obtained in the new bone

The comparisons between the two treatments on the new bone are presented in Table 2.

The mineral composition is modified after 12 months of treatment with ALN or SrRan. The evolution of all of the mineral PPVs in the new bone was different according to the treatment (all $p<0.001$) except for mineral maturity ($p=0.62$). The mineral/organic ratio (Raman) was increased by ALN but decreased during SrRan administration. The mineral/organic ratio (FTIRM) was increased by ALN but not modified by SrRan. Carbonation type B and carbonation (FTIRM) were not modified by ALN but were decreased by SrRan. The crystallinity (Raman and FTIRM) was increased by ALN and decreased by SrRan. The mineral maturity was not significantly modified regardless of the treatment.

The organic composition was not deeply modified by either treatment after 12 months in new bone. Two organic PPVs were significantly different between the two treatments: the hydroxyproline/proline ratio ($p=0.041$) and PG/AmideIII ($p<0.001$). The hydroxyproline/proline ratio was significantly increased by ALN and not modified by SrRan. PG/AmideIII was increased by ALN and decreased by SrRan in new bone within the same range. Collagen maturity (Raman and FTIRM) was not modified by either treatment in new bone after 12 months (Table 2).

The nanomechanical properties were not modified in new bone. The change in the nanomechanical PPV was not significantly different between the two treatments. The nanomechanical properties were not significantly modified in new bone by ALN or by SrRan treatment.

Interactions between treatment and location. Significant interactions were found between treatment and location (trabecular/cortical) in new bone for carbonation type B (Raman) ($p=0.040$) and mineral maturity (FTIRM) ($p=0.012$) only (Table 3). This result indicates that the effect of the treatment is a function of the location for both variables. A significant increase in carbonation type B was observed in cortical bone after ALN treatment but not in trabecular bone. In SrRan treatment, a significant decrease in carbonation type B was observed for cortical and trabecular bone. Mineral maturity was not modified in the cortical bone with ALN treatment but increased significantly in the cortical bone with SrRan treatment. Conversely, it decreased in the trabecular bone significantly with SrRan treatment but nonsignificantly with ALN treatment.

5.2 Comparison of the results obtained in the old bone

The comparisons between the two treatments in the old bone are presented in Table 4.

The mineral composition was modified in old bone by ALN but not by SrRan. The mineral/organic ratio (Raman) and crystallinity (Raman) were significantly increased in ALN old bone. The mineral PPVs were not modified by SrRan after 12 months of administration. No significant difference was found between the two treatments for the change in mineral PPVs in old bone.

The organic composition was modified in old bone by ALN and SrRan. In old bone, a significant difference was found between the 2 treatments for 2 variables: hydroxyproline/proline ratio ($p<0.001$) and PG/AmideIII ($p<0.001$). The hydroxyproline/proline ratio was significantly increased by both treatments, and the increase was lower with ALN than with SrRan. PG/AmideIII was not modified by ALN but was significantly decreased by SrRan administration. This variable was decreased within the same range in SrRan old bone as in SrRan new bone. The change in collagen maturity (Raman and FTIRM) was not significantly different between the two treatments, and no significant change was observed for either treatment.

The nanomechanical properties were not modified in old bone. No significant difference was found between the two treatments for the change in nanomechanical PPV in old bone.

Interactions between treatment and location. No significant interaction was found between treatment and location in old bone.

Table 2: Comparison of the changes in variables (ΔPPV) from baseline to 12 months between the two treatments in new bone. The mean ΔPPV and the statistical evaluation were calculated independently of the location of the bone (cortical and trabecular).

	mean ΔPPVs - new bone	ALN	SrRan	p-value
		Mean ΔPPV (95% CI)	Mean ΔPPV (95% CI)	
MINERAL	Mineral/Organic (Raman)	**+0.49 (+0.34 to +0.64)[a]**	**-0.27 (-0.42 to -0.13)[b]**	**<0.001**
	Mineral/Organic (FTIRM)	**+0.34 (+0.25 to +0.42) [b]**	+0.01 (-0.07 to +0.10)	**<0.001**
	Carbonation-type-B $\times 10^{-3}$ (Raman)	+1.67 (-0.21 to +3.54)	**-10.72 (-12.59 to -8.86)[a]**	**<0.001**
	Carbonation $\times 10^{-3}$ (FTIRM)	+0.25 (-0.08 to +0.57)	**-0.64 (-0.96 to -0.31)[a]**	**<0.001**
	Crystallinity $\times 10^{-3}$ (Raman)	**+0.82 (+0.61 to +1.01)[a]**	**-1.14 (-1.34 to -0.95)[a]**	**<0.001**
	Crystallinity $\times 10^{-3}$ (FTIRM)	**+0.86 (+0.44 to +1.29)[a]**	**-0.45 (-0.87 to -0.02)[c]**	**<0.001**
	Mineral maturity $\times 10^{-3}$ (FTIRM)	-9.53 (-86.15 to +67.08)	+17.43 (-59.18 to +94.05)	0.62
ORGANIC	HydroxyPro/Pro. $\times 10^{-3}$ (Raman)	**+8.66 (+2.13 to +15.18)[c]**	-1.06 (-7.56 to +5.43)	**0.041**
	Collagen maturity $\times 10^{-3}$ (Raman)	-11.06 (-25.11 to +2.99)	-7.25 (-21.23 to +6.73)	0.71
	Collagen maturity $\times 10^{-3}$ (FTIRM)	+60.01 (-98.02 to +218.00)	+90.65 (-67.39 to +248.70)	0.78
	PG/Amide III $\times 10^{-3}$ (Raman)	**+10.08 (+5.60 to +14.56)[a]**	**-9.33 (-13.80 to -4.87)[a]**	**<0.001**
NANO.	Elastic modulus (GPa)	+0.44 (-0.16 to +1.04)	+0.41 (-0.16 to +0.97)	0.93
	Tissue hardness (mPa)	+13.22 (-6.72 to +33.17)	+21.73 (+2.89 to +40.58)	0.53
	Working energy (pJ)	-83.24 (-214.45 to +47.97)	+17.28 (-106.26 to +140.84)	0.26
	Elastic energy (pJ)	-6.76 (-42.74 to +29.21)	+17.61 (-16.29 to +51.53)	0.32

The ΔPPV corresponds to the difference in the PPV between M0 and M12 adjusted on the PPV value at M0. The p-value corresponds to the comparison of the ΔPPV between the two treatments.
95% CI: 95% confidence interval
The labels a: p<0.001; b: p<0.01; c: p<0.05 correspond to the comparison of the ΔPPV with zero.

Table 3: Comparison of the changes in variables (ΔPPV) from baseline to 12 months between the two treatments according to a cortical or trabecular location in new bone. The effects of ALN and SrRan are functions of the location (cortical and trabecular) only for carbonation type B and mineral maturity. The other PPVs do not depend on the location.

	mean ΔPPVs - new bone	Location	ALN	SrRan	p-value
			Mean ΔPPV (95% CI)	Mean ΔPPV (95% CI)	
MINERAL	Carbonation-type-B $\times 10^{-3}$ (Raman)	Cortical	**+2.30 (+0.11 to +4.50)[c]**	**-11.86 (-14.08 to -9.64)[a]**	**0.040**
		Trabecular	+1.12 (-1.03 to +3.27)	**-9.73 (-11.84 to -7.61)[a]**	**0.040**
	Mineral maturity $\times 10^{-3}$ (FTIRM)	Cortical	+24.02 (-67.67 to +115.70)	**+143.6 (+51.13 to +236.0)[b]**	**0.012**
		Trabecular	-65.51 (-147.0 to +16.03)	**-86.30 (-167.1 to -5.49)[c]**	**0.012**

ΔPPV corresponds to the difference in the PPV between M0 and M12 adjusted on the PPV value at M0. The p-value corresponds to the comparison of the ΔPPV between the two treatments.

95% CI: 95% confidence interval

The labels a: p<0.001; b: p<0.01; c: p<0.05 correspond to the comparison of the ΔPPV with zero.

Table 4: Comparison of the changes in variables (ΔPPV) from baseline to 12 months between the two treatments in old bone. The mean ΔPPV and the statistical evaluation were calculated independently of the location of the bone (cortical and trabecular). Statistical analysis showed that the effects of ALN and SrRan are not a function of the location (cortical and trabecular) in old bone.

	mean ΔPPVs - old bone	ALN	SrRan	p-value
		Mean ΔPPV (95% CI)	Mean ΔPPV (95% CI)	
MINERAL	Mineral/Organic (Raman)	**+0.22 (+0.06 to +0.37)**	+0.11 (-0.04 to +0.27)	0.34
	Mineral/Organic (FTIRM)	+0.03 (-0.04 to +0.10)	+0.02 (-0.05 to +0.08)	0.76
	Carbonation-type-B $\times 10^{-3}$ (Raman)	-0.99 (-2.47 to +0.49)	+0.696 (-0.77 to +2.16)	0.11
	Carbonation $\times 10^{-3}$ (FTIRM)	-0.078 (-0.13 to +0.12)	-0.07 (-0.2 to +0.05)	0.48
	Crystallinity $\times 10^{-3}$ (Raman)	**+0.278 (+0.03 to +0.52)**	+0.041 (-0.2 to +0.29)	0.18
	Crystallinity $\times 10^{-3}$ (FTIRM)	+0.088 (-0.28 to +0.45)	-0.00043 (-0.37 to +0.37)	0.73
	Mineral maturity $\times 10^{-3}$ (FTIRM)	-12.15 (-74.38 to +50.07)	-24.63 (-86.85 to +37.60)	0.76
ORGANIC	Hydro./Pro. $\times 10^{-3}$ (Raman)	**+8.33 (+0.59 to +16.07)[c]**	**+30.77 (+23.06 to +38.47)[a]**	**<0.001**
	Collagen maturity $\times 10^{-3}$ (Raman)	-2.28 (-14.79 to +10.23)	-18.88 (-31.3 to -6.45)	0.06
	Collagen maturity $\times 10^{-3}$ (FTIRM)	-2.53 (-108.20 to +103.10)	+62.86 (-42.76 to +168.5)	0.38
	PG/AmideIII $\times 10^{-3}$ (Raman)	+1.25 (-1.45 to +3.94)	**-13.55 (-16.25 to -10.85)[a]**	**<0.001**
NANO.	Elastic modulus (GPa)	+0.43 (-0.24 to +1.10)	+0.94 (+0.30 to +1.58)	0.27
	Tissue hardness (mPa)	+17.21 (-13.48 to +47.90)	+39.71 (+10.59 to +68.91)	0.29
	Working energy (pJ)	+75.71 (-92.89 to +244.32)	+218.50 (+58.11 to +378.89)	0.22
	Elastic energy (pJ)	+38.41 (-32.5 to +109.33)	+74.13 (+6.69 to +141.57)	0.46

ΔPPV corresponds to the difference in the PPV between M0 and M12 adjusted on the PPV value at M0. The p-value corresponds to the comparison of the ΔPPV between the two treatments.

The labels a: p<0.001; b: p<0.01; c: p<0.05 correspond to the comparison of the ΔPPV with zero.

6 Discussion:

The aim of this study was to evaluate the differential effects of ALN and SrRan on bone quality in the short term at the ultrastructural level. The discussion is divided 2 sections. The first section discusses the results related to the new bone according to the mineral, organic matrix and nanomechanical properties. Similarly, the second section discusses the results related to old bone according to the mineral, organic matrix and nanomechanical properties.

6.1 Effects of ALN and SrRan on the new bone

ALN and SrRan had differential effects on the mineral composition of newly formed bone after 12 months of treatment. After 12 months of ALN treatment, the newly formed bone showed that the mineral/organic ratio, crystallinity, and type-B carbonate contents (cortical) were increased. This is in agreement with previous studies involving bisphosphonate treatments and vibrational spectroscopic techniques. ALN treatment (for 2-3 years) progressively increased mineralization in iliac bone biopsies from women with PMOP [5, 6]. A similar study evaluated the effect of zoledronate (ZOL) and teriparatide (TPTD) on mineral composition in human iliac bone biopsies after 6 months of administration [35]. The recently formed bone (cortical and trabecular) under ZOL administration had increased mineral/organic and crystallinity value compared to TPTD at similar bone ages. The effect of ALN on mineral composition was also studied for long-term treatment by Raman and FTIRM spectroscopy. The mineral composition of recently formed bone was not different between 3 and 5 years of ALN administration [9]. Similarly, administration of ALN for up to 10 years results in minimal and transient bone composition compared to treatment for 5 years [8]. Our results show that mineral recently formed under ALN administration are more mineralized and organized (showing increased crystallinity) compared to the baseline. ALN has an effect on the mineral composition within the first year of treatment compared to long-term treatment, probably due to the duration of administration. This finding was also observed for BPs other than ALN [36, 37].

Concerning the biopsies treated with SrRan, EDX imaging analysis confirmed the presence of Sr^{2+} in new bone, as previously reported [19, 38, 39]. The hydrated layer in new bone is larger than that in old bone [29]. The hydrated layer represents a pool of loosely bound ions that can be easily and rapidly exchanged with the surrounding environment. Thus, Sr^{2+} was found in new bone because it is easily captured in the hydrated layer of the new bone. The implication of the hydrated layer in the physicochemical mechanism of Sr^{2+} was also supported by the review of Marx *et al.*: “Sr treatment is more likely related to its interaction with collagen, water and the hydrated layer surrounding crystals,

rather than its ability to incorporate directly into HA" [13]. A decrease in the mineral/organic ratio after 12 months of SrRan administration was observed by Raman spectroscopy but not by FTIRM. A previous study concluded that Raman spectroscopy is more sensitive than FTIRM to the mineral/organic ratio in bone samples [40]. This result could explain the significant decrease detected by Raman spectroscopy but not by FTIRM. Carbonation (Raman and FTIRM) and crystallinity were decreased in new bone. To date, the effect of SrRan on the carbonate content in human bone has not been reported. This effect was only reported in studies involving biomaterials, bone from animal models or cell cultures [41-43]. The incorporation of 1.5% Sr^{2+} in synthetic hydroxyapatite (similar to the clinical dosage) did not change the composition of carbonate or the structure of the mineral [43]. The decrease in carbonation and crystallinity is not the result of the inclusion of Sr^{2+} in the mineral. The presence of Sr^{2+} reduced the crystal growth rates of hydroxyapatite in aqueous solution [44]. Thus, the presence of Sr^{2+} in the hydrated layer might induce a delay in the maturation process of the mineral. Therefore, the lower mineral/organic (Raman), crystallinity, carbonation and mineral maturity (trabecular) observed in new bone at M12 might also be a consequence of delayed maturation. In cortical bone, conversely, mineral maturity was increased at M12 in new bone, but the reason for this is unclear. Doublier *et al*. assessed mineral changes in bone biopsies from women with PMOP treated with SrRan for 3 years [X-ray diffraction and selected area electron diffraction (SAED)] [16]; SAED allows the distinction between new and old bone packets. No modification of crystallinity in new bone was found. Thus, delayed maturation might be a transitory effect within the first year.

The design of our study took into account the location of the bone (cortical and trabecular). In the new bone, 2 of 15 PPVs were found to be location dependent. In the literature, there is no clear hypothesis about the differential effect of antiresorptive treatment on cortical and trabecular bone composition. In a 2-year ibandronate administration study, the results showed that cortical and trabecular bone reacted similarly to the effect of the treatment, as assessed by qBEI [45]. After 3 years of ALN administration, the mineral/organic increased only in cortical bone, as assessed by FTIRM [6]. It is noteworthy that neither previous study took into account the differences in bone age. Concerning the effect of SrRan, a study of 10 paired biopsies showed that the amount of Sr was higher in new trabecular bone than in new cortical bone, as assessed by XRD and SAED [16]. The difference in the bone turnover rate between cortical and trabecular bone was proposed to explain the result. The absence of a clear hypothesis might be related to the nature of the measured variables (labile or bulk compound). In our study, the changes in carbonation type B and mineral maturity depended on the location (cortical or trabecular). Carbonation type B evaluates the relative amount of carbonate type B in the mineral.

458 Carbonate is known to be a labile compound in bone mineral [46]. Mineral maturity (FTIRM) evaluates
459 the relative amount of nonapatitic phosphate in bone mineral. Mineral maturity assesses the
460 transformation of immature precursors of the hydrated layer into mature apatite [12]. Thus, both
461 variables measure the relative amounts of labile compounds that are prone to be modified by the bone
462 turnover rate. Both variables are functions of the location because the bone turnover rate is different
463 between cortical and trabecular bone. The other variables (13/15) are not dependent on bone location
464 because they evaluate the relative amount of compound founds in the bulk matrix (or much less labile),
465 which are less prone to be modified by the bone turnover rate.
466 **The organic composition was not deeply modified by either treatment after 12 months in new bone.**
467 The organic matrix was assessed by FTIRM and Raman spectroscopy as 4 variables: collagen maturity
468 (FTIRM and Raman spectroscopy), hydroxyproline/proline ratio (Raman) and PG/amide III (Raman).
469 After 12 months of ALN treatment, collagen maturity was not modified in new bone (FTIRM and
470 Raman). The hydroxyproline/proline ratio was increased in new bone, revealing post-translational
471 modifications in collagen. The PG content (PG/AmideIII) increased significantly in new bone after 12
472 months of ALN. The relative PG content represents the noncollagenous compartment in bone. PGs play a
473 role in regulating mineralization by affecting apatite nucleation and growth [47]. For the short-term
474 treatment, the PG content was increased by ZOL compared to TPTD for 6 months of administration in
475 newly formed bone (cortical and trabecular) [35]. Our results are in agreement with the short-term
476 treatment. For long-term treatment of ALN, PG content in newly formed bone was not different between
477 human bone biopsies after 3, 5 or 10 years [8, 9]. This apparent discrepancy between short- and long-
478 term treatment might be due to the duration of administration. This result is not specific to ALN and was
479 also observed for other BPs [36, 37].
480 After 12 months of SrRan treatment, the collagen matrix was not modified in new bone. The
481 relative noncollagenous protein content (PG/AmideIII) was decreased in new bone. Recently, Marx *et al.*
482 suggested that Sr^{2+} can form bonds with collagenous and noncollagenous proteins (such as
483 proteoglycans) [13, 48]. The decrease in PG/amide III may result from the physicochemical effect of Sr^{2+}
484 on noncollagenous proteins.
485 **The nanomechanical properties are not modified by either treatment after 12 months in new bone.**
486 Previous studies have shown correlations between physicochemical parameters (Raman and FTIRM) and
487 nanomechanical properties [49, 50]. Correlations were observed in animal models as a function of bone
488 age. Mineral/organic, carbonation and crystallinity were found to increase with bone age. In our study,
489 the mineral and organic composition were modified in new bone by ALN and SrRan. However, the bone

nanomechanical properties were not modified in new bone by either treatment. The modification of the composition of bone might not be enough to induce a significant effect on the nanomechanical properties. Modifications of nanomechanical properties have previously only been observed after long-term treatment with BPs [37, 51].

6.2 Effects of ALN and SrRan on old bone

The mineral of old bone were modified by ALN but not by SrRan. The statistical analysis showed that the effect of each treatment was the same on cortical and trabecular old bone (Table 4). After 12 months of ALN treatment, the mineral/organic (Raman) and crystallinity (Raman) increased in old bone. The amplitude of the increases in old bone is lower than those in new bone. Even if it is old bone, bone packets continued to mineralize slowly [10]. Therefore, the low increase is the result of the slow mineralization of old bone packets. The increase, detected by Raman spectroscopy and not by FTIRM, is certainly due to the sensitivity of Raman spectroscopy, as discussed in section 6.1 [40].

After 12 months of SrRan treatment, the mineral PPVs were not modified. The old bone has a thin hydrated layer (compared to new bone); thus, Sr^{2+} was not adsorbed in the old bone mineral. As a consequence, SrRan did not modify the mineral composition of old bone. This result supported the hypothesis of a physicochemical mechanism of action of Sr^{2+}, which is related to the hydrated layer [13]. Moreover, it confirmed that modifications observed in mineral new bone were mainly related to the treatment and not artifacts of the embedding PMMA or long-term storage.

The organic matrix is modified in old bone by ALN and SrRan after 12 months of administration. After 12 months of ALN treatment, collagen maturity and the PG content were not modified in old bone (FTIRM and Raman). The hydroxyproline/proline ratio was increased in ALN old bone, suggesting post-translational modifications in collagen. This increase might also be related to the increase in mineralization in old bone, as observed in the mineral old bone [52].

After 12 months of SrRan treatment, collagen maturity was not modified in old bone. Hydroxyproline/proline was increased in old bone, revealing post-translational modification of collagen. The increase induced by SrRan was higher than that induced by ALN. The relative noncollagenous protein content (PG/AmideIII) was decreased in old bone. The Sr^{2+} can form bonds with collagenous and noncollagenous proteins (such as proteoglycans) [13, 48]. According to Frankaer *et al*., Sr^{2+} is fixed in both the mineral matrix and organic matrix [17]. These authors suggested the existence of inter- and intrafibrillar crosslinks in collagen. The increased hydroxyproline/proline and the decrease in PG/amide III may result from the physicochemical effect of Sr^{2+} on collagenous and noncollagenous proteins. This

strongly suggests a physicochemical mechanism of Sr^{2+}, more than a biological effect, since the modifications occur in both new and old bone.

The modifications of the physicochemical properties observed after 12 months of ALN or SrRan do not change the nanomechanical properties of old bone. Similar to new bone, the bone nanomechanical properties were not modified by ALN in old bone. The effects on bone nanomechanical properties have been previously observed only after long-term treatments with ALN [37, 53].

The effects of Sr on bone nanomechanical properties have mainly been investigated in animal models [39, 54, 55]. These studies revealed that the bone became harder, stiffer and tougher after treatment for 6 and 52 weeks. However, in bone biopsies from patients treated with SrRan for 3 years, the indentation modulus of the SrRan group was not different from that of the placebo group at similar bone ages [15]. Finally, the modifications of the composition (mineral or organic) induced in old bone by either ALN or SrRan after 12 months were too small to induce a significant effect on the bone nanomechanical properties.

7 Limitations and strengths

First, the location of new and old bone was based on the anatomical location (FTIRM and nanoindentation) and ESEM images (Raman). Therefore, data were assessed from bone samples that did not strictly have the same age. This sampling procedure may induce variability in the results that is not related to the effect of the molecule. Second, the analyses were performed with 3 different techniques. The locations probed by each technique were not strictly the same. However, an effort was made to analyze similar bone areas between the three different techniques. Third, iliac crest biopsies at M0 and M12 were performed on the same subject. We made the assumption that modifications induced by the embedding procedure and the storage conditions were equal for all biopsies. Moreover, we compared the PPVs at comparable bone ages to minimize the effect of age. Therefore, if there were differences in PPVs between M0 and M12, these differences were mainly related to the effect of the treatment, and the other effects were minimized.

Despite these limitations, the main results are consistent with those in the literature. This study capitalizes on 2 main strengths. The analyses were performed with 60 paired biopsies, a larger number than previous studies involving analyses of bone quality at the molecular level. Finally, each biopsy was represented by 40 repeated measurements per spectroscopic technique and 5 repeated measurements for nanoindentation, a larger number of measurements than previous studies to produce robust results.

8 Conclusions

The analysis of 60 paired biopsies from postmenopausal women receiving either ALN or SrRan for 12 months showed that both compounds modulated bone quality, particularly in newly formed bone, but in different fashions. ALN modulated bone quality through its antiresorptive action. The bone formed during 12 months of ALN is characterized by increased mineral content, carbonation and apatite crystal size/perfection. The nanomechanical properties were not modified after 12 months, likely due to the low modification of the bone composition induced by ALN or SrRan for 12 months. SrRan decreased the crystallinity/perfection of the crystals and the carbonate content due to its physicochemical mechanism of action. Sr^{2+} cations are captured in the mineral matrix by the hydrated layer and modify the molecular composition of bone at the level of the bone structural unit. The collagenic and noncollagenic matrices are modified in old bone. Sr^{2+} might form bonds (crosslinks) with collagen and noncollagenous proteins. Our results showed that ALN and SrRan have differential effects on bone quality in relation to their mechanism of action. Both drugs modified the mineral and organic compositions in their own fashion within the first 12 months of treatment.

9 Acknowledgements

The authors thank the Institut de Recherches Internationales Servier (Suresnes, France) for providing the samples for this study and for their financial support. We also thank P. Recourt (LOG UMR 8187, Villeneuve d'Ascq) for collecting the SEM images. The authors thank Guillaume Penel for his advice and help with this project.

10 Conflicts of interest

Dr Georges Boivin received grants and research support from Amgen, MSD, Servier. He was a consultant for Amgen, Servier. Delphine Farlay received grants and research support from Amgen and Servier. Dr Bernard Cortet received fees for occasional interventions as an expert or speaker for Amgen, Expanscience, Ferring, Lilly, Medtronic, MSD, Mylan, Novartis, Roche Diagnostics, Servier and UCB. The other co-authors do not have conflicts of interest to declare that are related to the present study.

11 CRediT authorship contribution statement

All authors read and approved the final version of the manuscript. Conceptualization and design: GF, DF, GB, PA. Acquisition of the data: GF, DF, CP, PA. Analysis and interpretation of the data: all authors. Statistical analysis: GF, HB. Writing-original draft: GF, DF. Writing-review and editing: GF, DF, GB, BC. Revising and final approval: GF, DF, GB, BC.

12 References

[1] M.D. Morris, G.S. Mandair, Raman assessment of bone quality, Clin. Orthop. Relat. Res. 469(8) (2011) 2160-9. 10.1007/s11999-010-1692-y

[2] C.V. Odvina, J.E. Zerwekh, D.S. Rao, N. Maalouf, F.A. Gottschalk, C.Y. Pak, Severely suppressed bone turnover: a potential complication of alendronate therapy, J. Clin. Endocrinol. Metab. 90(3) (2005) 1294-301. 10.1210/jc.2004-0952

[3] R. Russell, N. Watts, F. Ebetino, M. Rogers, Mechanisms of action of bisphosphonates: similarities and differences and their potential influence on clinical efficacy, Osteoporos. Int. 19(6) (2008) 733. 10.1007/s00198-007-0540-8

[4] R.G. Russell, Bisphosphonates: the first 40 years, Bone 49(1) (2011) 2-19. 10.1016/j.bone.2011.04.022

[5] G. Boivin, P.J. Meunier, Effects of bisphosphonates on matrix mineralization, J. Musculoskelet. Neuronal Interact. 2(6) (2002) 538-43.

[6] A.L. Boskey, L. Spevak, R.S. Weinstein, Spectroscopic markers of bone quality in alendronate-treated postmenopausal women, Osteoporos. Int. 20(5) (2009) 793-800. 10.1007/s00198-008-0725-9

[7] P. Roschger, S. Rinnerthaler, J. Yates, G.A. Rodan, P. Fratzl, K. Klaushofer, Alendronate increases degree and uniformity of mineralization in cancellous bone and decreases the porosity in cortical bone of osteoporotic women, Bone 29(2) (2001) 185.

[8] N. Hassler, S. Gamsjaeger, B. Hofstetter, W. Brozek, K. Klaushofer, E.P. Paschalis, Effects of long-term alendronate treatment on postmenopausal osteoporosis bone material properties, Osteoporos. Int. 26(1) (2015) 339-52. 10.1007/s00198-014-2929-5

[9] B. Hofstetter, S. Gamsjaeger, R.J. Phipps, R.R. Recker, F.H. Ebetino, K. Klaushofer, E.P. Paschalis, Effects of alendronate and risedronate on bone material properties in actively forming trabecular bone surfaces, J. Bone Miner. Res. 27(5) (2012) 995-1003. 10.1002/jbmr.1572

[10] P. Roschger, A. Lombardi, B.M. Misof, G. Maier, N. Fratzl-Zelman, P. Fratzl, K. Klaushofer, Mineralization density distribution of postmenopausal osteoporotic bone is restored to normal after long-term alendronate treatment: qBEI and sSAXS data from the fracture intervention trial long-term extension (FLEX), J. Bone Miner. Res. 25(1) (2010) 48-55. 10.1359/jbmr.090702

[11] E. Donnelly, D.S. Meredith, J.T. Nguyen, B.P. Gladnick, B.J. Rebolledo, A.D. Shaffer, D.G. Lorich, J.M. Lane, A.L. Boskey, Reduced cortical bone compositional heterogeneity with bisphosphonate treatment in postmenopausal women with intertrochanteric and subtrochanteric fractures, J. Bone Miner. Res. 27(3) (2012) 672-8. 10.1002/jbmr.560

[12] Y. Bala, B. Depalle, D. Farlay, T. Douillard, S. Meille, H. Follet, R. Chapurlat, J. Chevalier, G. Boivin, Bone micromechanical properties are compromised during long-term alendronate therapy independently of mineralization, J. Bone Miner. Res. 27(4) (2012) 825-34. 10.1002/jbmr.1501

[13] D. Marx, A. Rahimnejad Yazdi, M. Papini, M. Towler, A review of the latest insights into the mechanism of action of strontium in bone, Bone Rep 12 (2020) 100273. 10.1016/j.bonr.2020.100273

[14] C. Li, O. Paris, S. Siegel, P. Roschger, E.P. Paschalis, K. Klaushofer, P. Fratzl, Strontium is incorporated into mineral crystals only in newly formed bone during strontium ranelate treatment, J. Bone Miner. Res. 25(5) (2010) 968-75. 10.1359/jbmr.091038

[15] P. Roschger, I. Manjubala, N. Zoeger, F. Meirer, R. Simon, C. Li, N. Fratzl-Zelman, B.M. Misof, E.P. Paschalis, C. Streli, P. Fratzl, K. Klaushofer, Bone material quality in transiliac bone biopsies of postmenopausal osteoporotic women after 3 years of strontium ranelate treatment, J. Bone Miner. Res. 25(4) (2010) 891-900. 10.1359/jbmr.091028

[16] A. Doublier, D. Farlay, X. Jaurand, R. Vera, G. Boivin, Effects of strontium on the quality of bone apatite crystals: a paired biopsy study in postmenopausal osteoporotic women, Osteoporos. Int. 24(3) (2013) 1079-87. 10.1007/s00198-012-2181-9

[17] C.G. Frankaer, A.C. Raffalt, K. Stahl, Strontium localization in bone tissue studied by X-ray absorption spectroscopy, Calcif. Tissue Int. 94(2) (2014) 248-57. 10.1007/s00223-013-9806-7
[18] D. Bazin, A. Dessombz, C. Nguyen, H.K. Ea, F. Liote, J. Rehr, C. Chappard, S. Rouziere, D. Thiaudiere, S. Reguer, M. Daudon, The status of strontium in biological apatites: an XANES/EXAFS investigation, J Synchrotron Radiat 21(Pt 1) (2014) 136-42. 10.1107/S1600577513023771
[19] G. Boivin, D. Farlay, M.T. Khebbab, X. Jaurand, P.D. Delmas, P.J. Meunier, In osteoporotic women treated with strontium ranelate, strontium is located in bone formed during treatment with a maintained degree of mineralization, Osteoporos. Int. 21(4) (2010) 667-77. 10.1007/s00198-009-1005-z
[20] A. Doublier, D. Farlay, Y. Bala, G. Boivin, Strontium does not affect the intrinsic bone quality at tissue and BSU levels in iliac samples from Macaca fascicularis monkeys, Bone 64(0) (2014) 18-24. 10.1016/j.bone.2014.03.009
[21] P. Chavassieux, P.J. Meunier, J.P. Roux, N. Portero-Muzy, M. Pierre, R. Chapurlat, Bone histomorphometry of transiliac paired bone biopsies after 6 or 12 months of treatment with oral strontium ranelate in 387 osteoporotic women: randomized comparison to alendronate, J. Bone Miner. Res. 29(3) (2014) 618-28. 10.1002/jbmr.2074
[22] E.P. Paschalis, S. Gamsjaeger, K. Klaushofer, Vibrational spectroscopic techniques to assess bone quality, Osteoporos. Int. 28(8) (2017) 2275-2291. 10.1007/s00198-017-4019-y
[23] G. Falgayrac, B. Cortet, O. Devos, J. Barbillat, V. Pansini, A. Cotten, G. Pasquier, H. Migaud, G. Penel, Comparison of Two-Dimensional Fast Raman Imaging versus Point-by-Point Acquisition Mode for Human Bone Characterization, Analytical Chemistry 84(21) (2012) 9116-9123. 10.1021/ac301758y
[24] S. Schrof, P. Varga, L. Galvis, K. Raum, A. Masic, 3D Raman mapping of the collagen fibril orientation in human osteonal lamellae, J. Struct. Biol. (2014). 10.1016/j.jsb.2014.07.001
[25] T. Colard, G. Falgayrac, B. Bertrand, S. Naji, O. Devos, C. Balsack, Y. Delannoy, G. Penel, New Insights on the Composition and the Structure of the Acellular Extrinsic Fiber Cementum by Raman Analysis, PLoS One 11(12) (2016) e0167316. 10.1371/journal.pone.0167316
[26] C. Olejnik, G. Falgayrac, A. During, B. Cortet, G. Penel, Doses effects of zoledronic acid on mineral apatite and collagen quality of newly-formed bone in the rat's calvaria defect, Bone 89 (2016) 32-9. 10.1016/j.bone.2016.05.002
[27] S. Gamsjaeger, S.P. Robins, D.N. Tatakis, K. Klaushofer, E.P. Paschalis, Identification of Pyridinoline Trivalent Collagen Cross-Links by Raman Microspectroscopy, Calcif. Tissue Int. (2017). 10.1007/s00223-016-0232-5
[28] S. Gamsjaeger, W. Brozek, R. Recker, K. Klaushofer, E.P. Paschalis, Transmenopausal changes in trabecular bone quality, J. Bone Miner. Res. 29(3) (2014) 608-17. 10.1002/jbmr.2073
[29] D. Farlay, G. Panczer, C. Rey, P.D. Delmas, G. Boivin, Mineral maturity and crystallinity index are distinct characteristics of bone mineral, J. Bone Miner. Metab. 28(4) (2010) 433-45. 10.1007/s00774-009-0146-7
[30] D. Farlay, M.E. Duclos, E. Gineyts, C. Bertholon, S. Viguet-Carrin, J. Nallala, G.D. Sockalingum, D. Bertrand, T. Roger, D.J. Hartmann, R. Chapurlat, G. Boivin, The ratio 1660/1690 cm(-1) measured by infrared microspectroscopy is not specific of enzymatic collagen cross-links in bone tissue, PLoS One 6(12) (2011) e28736. 10.1371/journal.pone.0028736
[31] M. Gardegaront, D. Farlay, O. Peyruchaud, H. Follet, Automation of the Peak Fitting Method in Bone FTIR Microspectroscopy Spectrum Analysis: Human and Mice Bone Study, Journal of Spectroscopy 2018 (2018) 1-11. 10.1155/2018/4131029
[32] D. Farlay, G. Boivin, Bone Mineral Quality, in: Y. Dionyssiotis (Ed.), Osteoporosis, IntechOpen, Rijeka, 2012.
[33] P. Ammann, I. Badoud, S. Barraud, R. Dayer, R. Rizzoli, Strontium ranelate treatment improves trabecular and cortical intrinsic bone tissue quality, a determinant of bone strength, Journal of Bone and Mineral Research 22(9) (2007) 1419-1425. doi:10.1359/jbmr.070607

[34] P. Fratzl, H.S. Gupta, E.P. Paschalis, P. Roschger, Structure and mechanical quality of the collagen–mineral nano-composite in bone, J. Mater. Chem. 14(14) (2004) 2115-2123. 10.1039/b402005g
[35] E.P. Paschalis, D.W. Dempster, S. Gamsjaeger, S. Rokidi, N. Hassler, W. Brozek, F.W. Chan-Diehl, K. Klaushofer, K.A. Taylor, Mineral and organic matrix composition at bone forming surfaces in postmenopausal women with osteoporosis treated with either teriparatide or zoledronic acid, Bone 145 (2021) 115848. 10.1016/j.bone.2021.115848
[36] D. Ruffoni, P. Fratzl, P. Roschger, R. Phipps, K. Klaushofer, R. Weinkamer, Effect of temporal changes in bone turnover on the bone mineralization density distribution: a computer simulation study, J. Bone Miner. Res. 23(12) (2008) 1905-14. 10.1359/jbmr.080711
[37] B.M. Misof, N. Fratzl-Zelman, E.P. Paschalis, P. Roschger, K. Klaushofer, Long-term safety of antiresorptive treatment: bone material, matrix and mineralization aspects, Bonekey Rep 4 (2015) 634. 10.1038/bonekey.2015.1
[38] A. Doublier, D. Farlay, M.T. Khebbab, X. Jaurand, P.J. Meunier, G. Boivin, Distribution of strontium and mineralization in iliac bone biopsies from osteoporotic women treated long-term with strontium ranelate, Eur. J. Endocrinol. 165(3) (2011) 469-76. 10.1530/EJE-11-0415
[39] M. Cattani-Lorente, R. Rizzoli, P. Ammann, In vitro bone exposure to strontium improves bone material level properties, Acta Biomater. 9(6) (2013) 7005-13. 10.1016/j.actbio.2013.02.037
[40] M.J. Turunen, S. Saarakkala, L. Rieppo, H.J. Helminen, J.S. Jurvelin, H. Isaksson, Comparison Between Infrared and Raman Spectroscopic Analysis of Maturing Rabbit Cortical Bone, Appl. Spectrosc. 65(6) (2011) 595-603.
[41] A.L. Rossi, S. Moldovan, W. Querido, A. Rossi, J. Werckmann, O. Ersen, M. Farina, Effect of strontium ranelate on bone mineral: Analysis of nanoscale compositional changes, Micron 56 (2014) 29-36. 10.1016/j.micron.2013.09.008
[42] W. Querido, A.P. Campos, E.H. Martins Ferreira, R.A. San Gil, A.M. Rossi, M. Farina, Strontium ranelate changes the composition and crystal structure of the biological bone-like apatite produced in osteoblast cell cultures, Cell Tissue Res. (2014). 10.1007/s00441-014-1901-1
[43] Z.Y. Li, W.M. Lam, C. Yang, B. Xu, G.X. Ni, S.A. Abbah, K.M. Cheung, K.D. Luk, W.W. Lu, Chemical composition, crystal size and lattice structural changes after incorporation of strontium into biomimetic apatite, Biomaterials 28(7) (2007) 1452-60. 10.1016/j.biomaterials.2006.11.001
[44] S. Rokidi, P.G. Koutsoukos, Crystal growth of calcium phosphates from aqueous solutions in the presence of strontium, Chem. Eng. Sci. 77 (2012) 157-164. 10.1016/j.ces.2012.02.049
[45] B.M. Misof, J.M. Patsch, P. Roschger, C. Muschitz, S. Gamsjaeger, E.P. Paschalis, E. Prokop, K. Klaushofer, P. Pietschmann, H. Resch, Intravenous Treatment With Ibandronate Normalizes Bone Matrix Mineralization and Reduces Cortical Porosity After Two Years in Male Osteoporosis: A Paired Biopsy Study, J. Bone Miner. Res. 29(2) (2014) 440-449. 10.1002/jbmr.2035
[46] J.C. Elliott, Chapter 4 - Mineral, Synthetic and Biological Carbonate Apatites, in: J.C. Elliott (Ed.), Studies in Inorganic Chemistry, Elsevier1994, pp. 191-304.
[47] D.B. Burr, O. Akkus, Bone Morphology and Organization, in: D.B.B.R. Allen (Ed.), Basic and Applied Bone Biology, Academic Press, San Diego, 2014, pp. 3-25.
[48] J.B. Thompson, J.H. Kindt, B. Drake, H.G. Hansma, D.E. Morse, P.K. Hansma, Bone indentation recovery time correlates with bond reforming time, Nature 414(6865) (2001) 773-6. 10.1038/414773a
[49] E. Donnelly, A.L. Boskey, S.P. Baker, M.C. van der Meulen, Effects of tissue age on bone tissue material composition and nanomechanical properties in the rat cortex, J. Biomed. Mater. Res. A 92(3) (2010) 1048-56. 10.1002/jbm.a.32442
[50] S. Gourion-Arsiquaud, J.C. Burket, L.M. Havill, E. DiCarlo, S.B. Doty, R. Mendelsohn, M.C. van der Meulen, A.L. Boskey, Spatial variation in osteonal bone properties relative to tissue and animal age, J. Bone Miner. Res. 24(7) (2009) 1271-81. 10.1359/jbmr.090201

723 [51] C.K. Tjhia, S.M. Stover, D.S. Rao, C.V. Odvina, D.P. Fyhrie, Relating micromechanical properties and
724 mineral densities in severely suppressed bone turnover patients, osteoporotic patients, and normal
725 subjects, Bone 51(1) (2012) 114-122. 10.1016/j.bone.2012.04.010
726 [52] K. Buckley, P. Matousek, A.W. Parker, A.E. Goodship, Raman spectroscopy reveals differences in
727 collagen secondary structure which relate to the levels of mineralisation in bones that have evolved for
728 different functions, J. Raman Spectrosc. 43(9) (2012) 1237-1243. 10.1002/jrs.4038
729 [53] C.K. Tjhia, S.M. Stover, D.S. Rao, C.V. Odvina, D.P. Fyhrie, Relating micromechanical properties and
730 mineral densities in severely suppressed bone turnover patients, osteoporotic patients, and normal
731 subjects, Bone 51(1) (2012) 114-22. 10.1016/j.bone.2012.04.010
732 [54] D.G. Yu, H.F. Ding, Y.Q. Mao, M. Liu, B. Yu, X. Zhao, X.Q. Wang, Y. Li, G.W. Liu, S.B. Nie, S. Liu, Z.A.
733 Zhu, Strontium ranelate reduces cartilage degeneration and subchondral bone remodeling in rat
734 osteoarthritis model, Acta Pharmacol. Sin. 34(3) (2013) 393-402. 10.1038/aps.2012.167
735 [55] S.D. Bain, C. Jerome, V. Shen, I. Dupin-Roger, P. Ammann, Strontium ranelate improves bone
736 strength in ovariectomized rat by positively influencing bone resistance determinants, Osteoporos. Int.
737 20(8) (2009) 1417-28. 10.1007/s00198-008-0815-8
738
739